

# Rapid annealing of the vacancy-oxygen center and the divacancy center by diffusing hydrogen in silicon

J. H. Bleka,<sup>1,\*</sup> I. Pintilie,<sup>2</sup> E. V. Monakhov,<sup>1</sup> B. S. Avset,<sup>3</sup> and B. G. Svensson<sup>1</sup><sup>1</sup>Department of Physics, Physical Electronics, University of Oslo, P.O. Box 1048 Blindern, N-0316 Oslo, Norway<sup>2</sup>Institute for Experimental Physics, Hamburg University, D-22761 Hamburg, Germany  
and National Institute of Materials Physics, Bucharest-Magurele 077125, Romania<sup>3</sup>Microsystems and Nanotechnology, SINTEF ICT, P.O. Box 124 Blindern, N-0314 Oslo, Norway

(Received 5 September 2007; revised manuscript received 2 November 2007; published 26 February 2008)

In hydrogenated high-purity Si, the vacancy-oxygen (VO) center is shown to anneal already at temperatures below 200 °C and is replaced by a center, identified as a vacancy-oxygen-hydrogen complex, with an energy level 0.37 eV below the conduction-band edge and a rather low thermal stability. At long annealing times, the process is reversed and the concentration of the latter defect is reduced, while the VO center partly recovers. The divacancy ( $V_2$ ) center anneals in parallel with the initial annealing of the VO center, and the loss in  $V_2$  exhibits a one-to-one proportionality with the appearance of a hole trap 0.23 eV above the valence-band edge attributed to a divacancy-hydrogen ( $V_2H$ ) center.

DOI: 10.1103/PhysRevB.77.073206

PACS number(s): 71.55.Cn, 66.30.J-, 61.80.Fe

Hydrogen in Si readily reacts with vacancy-type defects by passivating the dangling bonds. It is known, for instance, that the vacancy-oxygen (VO) center and the divacancy ( $V_2$ ) center disappear at low temperatures in the presence of hydrogen.<sup>1</sup> The VO center is believed to be transformed into a VOH center,<sup>2–10</sup> while the annealing mechanism for the  $V_2$  center is less documented. Evidence for the existence of a  $V_2H$  center has been obtained by electron-paramagnetic-resonance measurements,<sup>2</sup> and based mainly on comparison of the threshold temperatures during isochronal annealing of  $V_2$  and  $V_2H$ , a level at about  $E_c - 0.43$  eV ( $E_c$  being the energy of an electron at the conduction-band edge) has been tentatively assigned to  $V_2H$ .<sup>9</sup>

Further, in contrast to the diffusion of molecular hydrogen, where the activation energy was firmly established ten years ago,<sup>11</sup> the diffusivity of monatomic hydrogen has been more difficult to determine. Reported values for the migration energy of monatomic hydrogen range from 0.48 eV (Ref. 12) to 1.2 eV (Ref. 13) and, presumably, depend on the charge state of the hydrogen. Recently, it has been shown that the lower value of these activation energies is close to that of the diffusivity of protons.<sup>14</sup>

In the present work, hydrogen-assisted annealing of vacancy-type defects in irradiated high-purity Si is studied, by deep-level transient spectroscopy (DLTS), to reveal which mechanisms are present and to clarify which form of hydrogen is involved during different annealing stages.

The samples investigated were  $p^+n^-n^+$  Si diodes produced from high-purity detector-grade magnetic-Czochralski wafers with a phosphorous concentration of  $5 \times 10^{12} \text{ cm}^{-3}$ . Hydrogen was introduced by submerging the samples in 10% hydrofluoric acid at 50 °C for  $\frac{1}{2}$  h. Aluminum contacts were deposited before irradiation at room temperature (RT) with 6-MeV electrons to a dose of  $5 \times 10^{12} \text{ cm}^{-2}$ . The concentrations of oxygen and carbon were found, by secondary-ion mass spectrometry, to be  $(0.5-1) \times 10^{18} \text{ cm}^{-3}$  and  $\leq 10^{16} \text{ cm}^{-3}$ , respectively. The setup used for the DLTS measurements is a refined version of one described elsewhere.<sup>15</sup>

Figure 1 shows the results of DLTS measurements for a

hydrogenated sample measured prior to and after three different annealing times at 195 °C. The DLTS spectrum recorded after the electron irradiation shows three major peaks related to the VO center and the  $V_2$  center. A peak labeled  $E1$ , which is not detectable in nonhydrogenated control samples, is seen as a small shoulder on the  $V_2(-/0)$  peak. Here, it is important to emphasize that  $E1$  should not be confused with the level referred to as  $E4$  and recently discussed in detail in Ref. 16. Despite having almost identical DLTS signatures,  $E1$  and  $E4$  originate from different defects;  $E4$  is unstable already at RT and occurs with the same concentration irrespective of the hydrogen content, in direct contrast to that of  $E1$  which does not appear in nonhydrogenated control samples. In fact,  $E4$  was found to disappear in the studied hydrogenated samples long time (up to nine months storage at RT) before the annealing at elevated temperatures was undertaken. Moreover, the  $E4$  level is never observed without a corresponding energy level at  $E_c - 0.45$  eV; this

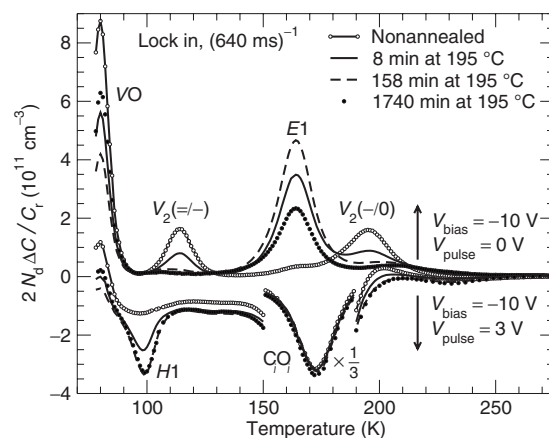


FIG. 1. DLTS spectra at four different annealing stages of a hydrogenated sample measured with ( $V_{\text{pulse}}=3$  V) and without ( $V_{\text{pulse}}=0$  V) forward injection. An estimate for the trap concentration, which does not account for the so-called lambda effect, can be read out at each of the peaks (Ref. 17).

level appears with the same concentration as  $E4$ , indicating that the complex causing  $E4$ , unlike the  $E1$  center, has two charge states in the upper half of the band gap.<sup>16</sup> All four DLTS spectra in Fig. 1 measured with forward injection show the presence of a major hole trap identified as the interstitial-carbon–interstitial-oxygen ( $C_iO_i$ ) center. After the initial 8-min anneal, the concentration of the VO center ( $[VO]$ ) has decreased by 35% and the  $E1$  peak has grown with an amplitude similar to the reduction of the VO peak. The concentration of the  $V_2$  center ( $[V_2]$ ) has dropped by 55%, concurrent with the appearance of the hole trap labeled  $H1$ . It should be pointed out that nonhydrogenated control samples show no annealing of the VO center and  $V_2$  center during the anneals up to 200 °C.

The  $E1$  level is found at  $E_c - 0.37$  eV and has an apparent electron capture cross section of  $8 \times 10^{-15}$  cm<sup>2</sup>. The energy level measured for the  $H1$  center is found to be at  $E_v + 0.23$  eV ( $E_v$  being the energy of an electron at the top of the valence band) with an apparent hole capture cross section of  $1 \times 10^{-13}$  cm<sup>2</sup>.

By employing a concept outlined by Hallén *et al.*<sup>18</sup> involving minority-carrier injection and a double-pulse sequence for majority carriers, the  $H1$  center was found to exhibit an effective hole capture cross section several orders of magnitude larger than that for electrons ( $10^{-14}$  cm<sup>2</sup> versus  $10^{-19}$  cm<sup>2</sup> at 100 K). These values suggest a complete occupation of the  $H1$  center during DLTS measurements with forward injection, resulting in a direct correspondence of the amplitude of the  $H1$  peak with the concentration of  $H1$  centers.

The trends continue as the hydrogenated sample is annealed for 158 min: The loss in  $[VO]$  is similar to the gain in  $[E1]$ , and the loss in  $[V_2]$  is similar to the further increase in  $[H1]$ . After the sample has been annealed for 1740 min,  $[VO]$  has recovered by  $\sim 50\%$  from the 158-min anneal and a similar loss is seen for  $[E1]$ . The apparent transformation of  $V_2$  to  $H1$  is completed after the 158-min anneal, and within the experimental accuracy, no further changes are observed after the 1740-min anneal.

Figure 2 shows the concentration of the various defects as a function of time in two hydrogenated samples annealed isothermally at 150 and 195 °C, respectively. Similar annealing behavior is seen at both temperatures:  $[VO]$  is reduced at a high rate initially, but is partly recovered after longer annealing times, and  $[V_2]$  is reduced at an even higher relative rate compared to  $[VO]$  in the early stage, and continues to decrease at a lower rate in the stages where  $[VO]$  has ceased to decrease. The sum of  $[VO]$  and  $[E1]$  is constant, within the experimental accuracy. For the sample annealed at 195 °C,  $[H1]$  was also measured and the sum of  $[V_2]$  and  $[H1]$  remains constant, within the experimental accuracy.  $[H1]$  is taken as the value at the  $H1$  peak subtracted by the background signal in this temperature range. The appearance of the  $H1$  center has also been detected during isochronal annealing studies at temperatures below 195 °C and a similar correlation to  $[V_2]$  is observed.<sup>19</sup>

The close one-to-one proportionality between the variations in  $[VO]$  and  $[E1]$ , and  $[V_2]$  and  $[H1]$ , is also illustrated in Fig. 3, where the gain in  $[E1]$  and  $[H1]$  is shown as a

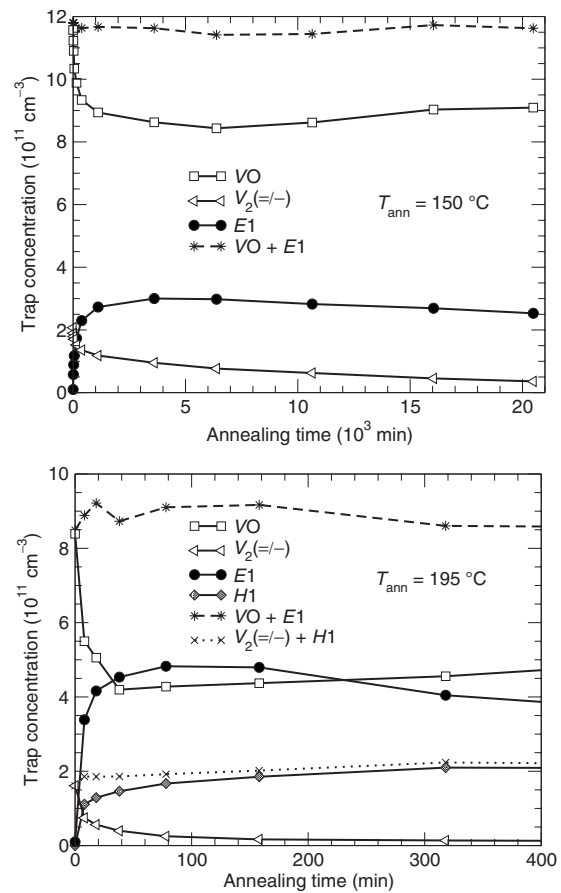


FIG. 2. Time dependence of the defect concentrations in two samples annealed isothermally at 150 and 195 °C (the sample from Fig. 1), respectively.  $[H1]$  is measured only for the latter.

function of the loss in  $[VO]$  and  $[V_2]$ , respectively. The data points of  $[E1]$  versus  $[VO]$  appear close to the line  $y=x$  for both temperatures as  $[E1]$  first increases and later decreases. The figure also shows that the appearance of the  $H1$  center

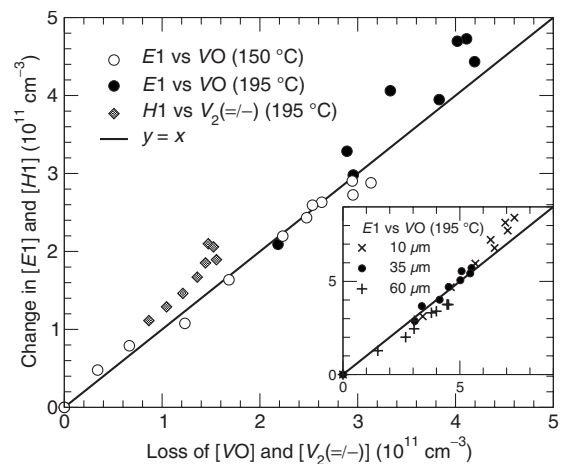


FIG. 3. Correlation of the change in  $[E1]$  and  $[H1]$  to the loss in  $[VO]$  and  $[V_2]$ , respectively. The concentrations are from Fig. 2. The inset has axes units identical to those of the main graph and shows the correlation of the change in  $[E1]$  to the loss in  $[VO]$  deduced from depth profiles (see Fig. 5) at three different depths.

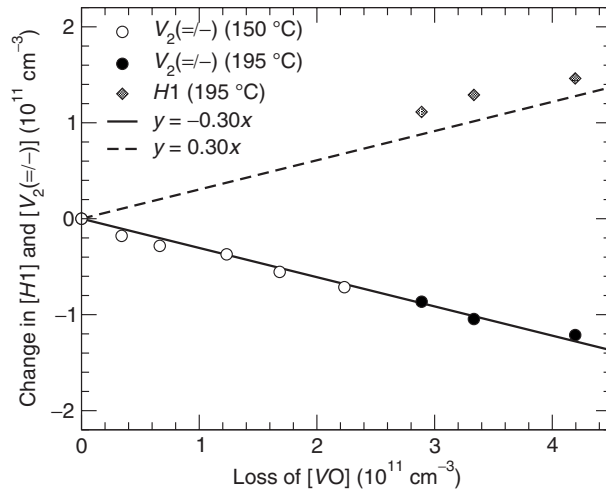


FIG. 4. Correlation of the change in  $[H1]$  and  $[V_2]$  to the loss in  $[VO]$  (concentrations from Fig. 2). The solid line is fitted to the  $V_2$  points. The broken line is a reflection of the solid one.

has a correlation to the disappearance of the  $V_2$  center, which is nearly one to one. The concentrations in this plot are extracted from the DLTS signal and are, thus, weighted averages of the defect concentrations between the depletion depths with  $V_{\text{bias}}=0$  V and  $V_{\text{bias}}=-10$  V, respectively. The correlation between  $[E1]$  and  $[VO]$  shown in the inset is derived from concentrations measured at specific depths, and it shows a similar picture as that obtained from the weighted average of the defect concentrations.

Figure 4 shows the change in  $[H1]$  and  $[V_2]$  versus the loss in  $[VO]$  during the initial stage of the annealing. The losses in  $[V_2]$  and  $[VO]$  are correlated, and the data can be closely fitted by the line  $y=-0.30x$ . The data points of  $[H1]$  versus  $[VO]$  lie close to the line  $y=0.30x$ . The small deviation from this line is within the experimental uncertainty, but is practically constant and may be due to an uncertainty in the DLTS background.

The initial value of  $[VO]$  is a factor of 5.2 larger than that of  $[V_2]$ . If the  $VO$  center and the  $V_2$  center anneal with the same relative rate, the data for the change in  $[V_2]$  versus that in  $[VO]$  should follow a line with the slope  $(5.2)^{-1}=0.19$  (cf. 0.30 in Fig. 4). Isochronal annealing of samples similar to those used in this study shows that the  $V_2$  center anneals out together with the  $VO$  center, but at a slightly higher relative rate, for all temperatures in the range from 100 to 225 °C.<sup>19</sup> It is, therefore, reasonable to assume that the  $VO$  center and the  $V_2$  center interact with the same migrating species, but with different probabilities. Since this difference in probability is, as revealed in Fig. 4, independent of the annealing temperature, it is most likely caused by a difference in capture radius rather than in reaction barrier. The observations can be explained by the  $V_2$  center having a capture radius  $0.30/0.19 \approx 1.6$  times that of the  $VO$  center, which seems plausible considering the geometrical size of the two defects.

Figure 5 displays the depth profiles, corrected for the lambda effect, of  $[VO]$ ,  $[E1]$ , and  $[V_2]$  at each of the four annealing steps shown in Fig. 1. In the nonannealed state after the electron irradiation,  $[E1]$  is too low for a depth

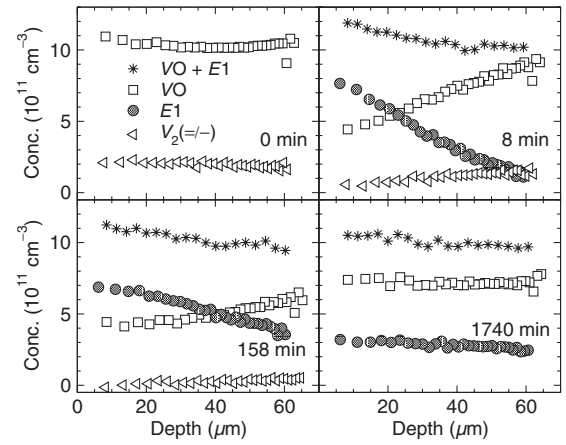


FIG. 5. Depth profiles of the four major electron traps at each of the annealing steps (195 °C) shown in Fig. 1.

profile to be measured. The absence of hydrogen-related peaks (such as, e.g.,  $E1$  and  $VOH$ ) does, however, show that the hydrogen is mainly located shallower than the zero-bias depletion width ( $\sim 5 \mu\text{m}$ ). After the 8-min anneal,  $[VO]$  and  $[V_2]$  are reduced in the near-surface region, while  $[E1]$  increases toward the surface. The sum of the profiles of  $[VO]$  and  $[E1]$  after the 8-min annealing step is similar to the profile of  $[VO]$  before the annealing; this suggests strongly that a certain configuration of hydrogen,  $H_x$ , is released at the surface of the sample and diffuses into the bulk, causing the reactions  $VO+H_x \rightarrow VOH_x$  and  $V_2+H_x \rightarrow V_2H_x$ , where  $E1$  is identified as  $VOH_x$ . The signal from the  $V_2$  center is rather weak already after the 8-min anneal, but it is evident that the profile of  $[V_2]$  also decreases toward the surface, possibly with a slightly higher relative rate than that of the  $VO$  center (which is expected to be the case if the  $V_2$  center has a larger capture radius for  $H_x$ ).

The depth profiles measured after annealing for 158 min show that more hydrogen has entered the sample from the front-surface side and more  $VO$  centers are transformed into  $E1$  centers.  $[V_2]$  is hardly measurable at this stage.

Annealing for 1740 min causes  $VOH_x$  to break up in the reaction  $VOH_x \rightarrow VO+H_x$ .  $[E1]$  is reduced at all depths, while the sum of  $[VO]$  and  $[E1]$  is still similar to the initial  $[VO]$ . Thus,  $VOH_x$  is rather unstable and appears to have a high concentration only as long as there is a large supply of  $H_x$ . The latter consideration is further supported by the annealing behavior of the  $V_2$  center as the dissociation of  $VOH_x$  constitutes a source of  $H_x$ . As a result, annealing of the  $V_2$  center continues after the  $H_x$  surface source is exhausted and the annealing of the  $VO$  center has ceased (see Fig. 2).

The diffusion coefficient of molecular hydrogen ( $H_2$ ) is reported to have an activation energy of  $(0.78 \pm 0.05)$  eV with a preexponential factor of  $(2.6 \pm 1.5) \times 10^{-4} \text{ cm}^2/\text{s}$ .<sup>11</sup> Assuming a one-dimensional diffusion of  $H_2$  from the surface at 195 °C shows that an unphysical amount ( $\gg 10^{300} \text{ cm}^{-2}$ ) of  $H_2$  is required in the surface region to obtain a concentration of  $10^{12} \text{ cm}^{-3}$  at a depth of  $30 \mu\text{m}$ . In addition,  $VOH_2$  is, from theoretical work, expected to be electrically inactive.<sup>10</sup> Hence, an identification of  $H_x$  as  $H_2$  does not appear to be likely.

On the other hand, the one-dimensional diffusion model shows that if the diffusivity of protons is assumed, monatomic hydrogen is sufficiently mobile to provide the amount of hydrogen required to account for the profiles in Fig. 5. Atomic hydrogen is known to interact with the VO center and form the well-established VOH center.<sup>2–10</sup> VOH exhibits a rather high stability ( $\sim 350^\circ\text{C}$ ) and gives rise to one acceptorlike level at  $\sim 0.32$  eV below  $E_c$  and one donorlike level at  $\sim 0.28$  eV above  $E_v$ . Levels with such positions and thermal properties are not found in this study and, hence,  $E1$  cannot be ascribed to the previously established VOH center. The most consistent interpretation seems to be that  $H_x$  is positively charged monatomic hydrogen, which combines with the VO center to form a complex with an atomic configuration different from that of the established VOH center. Thus, the  $E1$  center is assigned to a  $\text{VOH}^*$  center, being a more unstable configuration than VOH. This assignment implies that the established reaction causing hydrogen and VO to combine into the VOH center must have a formation barrier larger than that of the  $\text{VOH}^*$  center. This is consistent with the fact that the formation of the VOH center normally occurs at higher temperatures than the ones used in the present study. The assignment of  $H_x$  to atomic hydrogen is further supported by the fact that the boron-hydrogen center in the  $p^+$  layer is anticipated to release monatomic hydrogen at  $\sim 100^\circ\text{C}$ .<sup>20</sup>

Our results provide clear evidence that the VO center and the  $V_2$  center anneal through interaction with the same species, and if  $H_x$  is monatomic hydrogen, the hydrogen-driven annealing of the  $V_2$  center is expected to result in the  $V_2\text{H}$  center through the reaction  $V_2 + \text{H} \rightarrow V_2\text{H}$ . It has been speculated that the  $V_2\text{H}$  center has a level at  $\sim 0.43$  eV below  $E_c$ ,<sup>2,9</sup> but this level is not observed in the present study. In fact, the close one-to-one proportionality between the loss in  $[V_2]$  and the increase in  $[H1]$  strongly favors an assignment of  $H1$  to  $V_2\text{H}$ . This implies that  $V_2\text{H}$  has only a donor level in the band gap, which is in direct contrast to  $V_2$  having two

acceptor levels and one donor level in the band gap:  $V_2(=/-)$  at  $E_c - 0.23$  eV,  $V_2(-/0)$  at  $E_c - 0.43$  eV, and  $V_2(0/+)$  at  $E_v + 0.19$  eV.  $V_2(0/+)$  cannot be observed by performing DLTS with hole injection, because the capture cross section for electrons is considerably larger than that for holes, resulting in a very low hole occupancy of this charge state.<sup>18</sup> When a hydrogen atom is captured by the  $V_2$  center, it is believed to partially passivate the center, causing the disappearance of the  $(=/-)$  transition, while the  $(-/0)$  transition remains. Thus,  $V_2\text{H}$  may be expected to have two levels:  $V_2\text{H}(-/0)$  and  $V_2\text{H}(0/+)$ , with activation energies similar to the corresponding ones of  $V_2$ . The interpretation of the present results is partially in disagreement with this picture: The  $V_2\text{H}(0/+)$  level, at  $E_v + 0.23$  eV, is similar to  $V_2(0/+)$ , but a  $V_2\text{H}(-/0)$  level is not observed. It should also be pointed out that the  $H1$  level, unlike  $V_2(0/+)$ , can be saturated with forward-injection DLTS; this supports a modified atomic configuration of  $V_2\text{H}$  compared to that of  $V_2$ .

In summary, a hydrogen-mediated annealing mechanism, acting at low temperature, for the VO center and the  $V_2$  center has been revealed. A one-to-one proportionality is found between the changes in  $[VO]$  and  $[E1]$ . The  $E1$  center gives rise to a level at  $E_c - 0.37$  eV, and is identified as a vacancy-oxygen center with a loosely bound hydrogen atom ( $\text{VOH}^*$ ). As the hydrogen supply is exhausted, this center breaks up and  $[VO]$  partly recovers. We have also found a one-to-one proportionality between the loss in  $[V_2]$  and the growth of a hole trap at  $E_v + 0.23$  eV (labeled  $H1$ ). It is suggested that the  $H1$  level originates from a  $V_2\text{H}$  center, although the electrical properties of the latter are in disagreement with assignments made in previous reports.

Financial support by the Norwegian Research Council is greatly appreciated. One of the authors (I.P.) thanks the Alexander von Humboldt Foundation for enabling her participation in this work.

\*janhb@fys.uio.no

<sup>1</sup>E. V. Monakhov, A. Ulyashin, G. Alfieri, A. Yu. Kuznetsov, B. S. Avset, and B. G. Svensson, Phys. Rev. B **69**, 153202 (2004).

<sup>2</sup>K. Bonde Nielsen, L. Dobaczewski, K. Goscinski, R. Bendesen, Ole Andersen, and B. Bech Nielsen, Physica B **273–274**, 167 (1999).

<sup>3</sup>B. G. Svensson, A. Hallén, and B. U. R. Sundqvist, Mater. Sci. Eng., B **4**, 285 (1989).

<sup>4</sup>K. Irmscher, H. Klose, and K. Maass, J. Phys. C **17**, 6317 (1984).

<sup>5</sup>A. R. Peaker, J. H. Evans-Freeman, P. Y. Y. Kan, L. Rubaldo, I. D. Hawkins, K. D. Vernon-Parry, and L. Dobaczewski, Physica B **273–274**, 243 (1999).

<sup>6</sup>Y. Tokuda and T. Seki, Semicond. Sci. Technol. **15**, 126 (2000).

<sup>7</sup>P. Lévêque, P. Pellegrino, A. Hallén, B. G. Svensson, and V. Privitera, Nucl. Instrum. Methods Phys. Res. B **174**, 297 (2001).

<sup>8</sup>P. Pellegrino, P. Lévêque, J. Lalita, A. Hallén, C. Jagadish, and B. G. Svensson, Phys. Rev. B **64**, 195211 (2001).

<sup>9</sup>P. Lévêque, A. Hallén, B. G. Svensson, J. Wong-Leung, C. Jagadish, and V. Privitera, Eur. Phys. J.: Appl. Phys. **23**, 5 (2003).

<sup>10</sup>J. Coutinho, O. Andersen, L. Dobaczewski, K. Bonde Nielsen,

A. R. Peaker, R. Jones, S. Öberg, and P. R. Briddon, Phys. Rev. B **68**, 184106 (2003).

<sup>11</sup>V. P. Markevich and M. Suezawa, J. Appl. Phys. **83**, 2988 (1998); C. Herring and N. M. Johnson, *ibid.* **87**, 4635 (2000); V. P. Markevich and M. Suezawa, *ibid.* **87**, 4637 (2000).

<sup>12</sup>A. Van Wieringen and N. Warmoltz, Physica (Amsterdam) **22**, 849 (1956).

<sup>13</sup>R. C. Newman, J. H. Tucker, A. R. Brown, and S. A. McQuaid, J. Appl. Phys. **70**, 3061 (1991).

<sup>14</sup>J. Weber, S. Knack, O. V. Feklisova, N. A. Yarykin, and E. B. Yakimov, Microelectron. Eng. **66**, 320 (2003).

<sup>15</sup>B. G. Svensson, K.-H. Rydén, and B. M. S. Lewerentz, J. Appl. Phys. **66**, 1699 (1989).

<sup>16</sup>J. H. Bleka, E. V. Monakhov, B. G. Svensson, and B. S. Avset, Phys. Rev. B **76**, 233204 (2007).

<sup>17</sup>D. V. Lang, J. Appl. Phys. **45**, 3023 (1974).

<sup>18</sup>A. Hallén, N. Keskitalo, F. Masszi, and V. Nágel, J. Appl. Phys. **79**, 3906 (1996).

<sup>19</sup>J. H. Bleka (unpublished).

<sup>20</sup>T. Zundel and J. Weber, Phys. Rev. B **39**, 13549 (1989).